ADAPTIVE DIGITAL CONTROL SYSTEM OF FLOW RATES FOR AN OTEC PLANT

Masatoshi **NAKAMURA*** and Haruo **UEHARA****

* Department of Electrical Engineering, Saga University, Honjomachi, Saga 840, Japan

** Department of Mechanical Engineering, Saga University, Honjomachi, Saga 840, Japan

Abstract: The purpose of ocean thermal energy conversion (OTEC) plant control is to provide stable power efficiently by appropriately regulating the seawater flow rates and the working fluid flow rate under conditions of continually changing seawater temperatures. This paper describes digital control of working fluid flow rate based on an adaptive control theory for the "Imari 2" OTEC plant at Saga University. Provisions have been made for linkage between the software of the adaptive control theory and the hardware of the OTEC plant. In implementing the working fluid flow rate control, if persistency of excitation conditions are lost, the algorithm of identification often exhibits bursting phenomena. To avoid this difficulty, the stopping-and-starting rule for identification was derived and was used for the working fluid flow rate control. Satisfactory control performance was then obtained by using this digital control system.

1. Introduction

The principle of ocean thermal energy conversion (OTEC) is to extract power from temperature differences existing in the oceans [1]. Because the thermal efficiency in OTEC plants is generally low, on the order of 3 percent, and the operating conditions, such as seawater temperatures, are constantly changing [2],[3], the role of control is of great importance in operating an OTEC plant effectively [4]. Among the many control theories, adaptive control is the most promising for this purpose. The adaptive control theory gives a control algorithm which tunes its parameter on-line for the plant [5],[6].

We constructed the digital control system of working fluid flow rate for the "Imari 2" OTEC plant at Saga University [7]. In the construction of the system, provision was made for linkage between the software of control theories and the hardware of the OTEC plant. This paper treats the problem of identification bursting phenomena during periods of the absence of persistency of excitation. To circumvent this difficulty, the stopping-and-starting rule for identification is derived and is used for the working fluid flow rate control. We obtained satisfactory control performance using this digital control system.

This paper is organized as follows: in section 2, we review the digital control system of working fluid flow rate; then, in section 3, we explain identification bursting phenomena and derive the stopping-and-starting rule for identification to avoid the difficulty; and finally, in section 4, discuss the feature of this study.

2. Design of Digital Control System

2.1 OTEC plant and control objective

The closed cycle OTEC plant, shown in Fig. 1, consists of an evaporator, condenser, turbine-

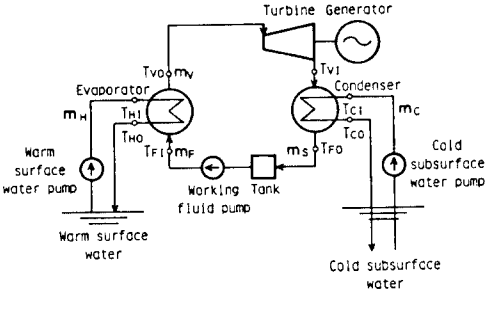

Fig. 1 Scheme for closed cycle OTEC plant

Fig. 2 The entire view of the "Imari 2" OTEC plant

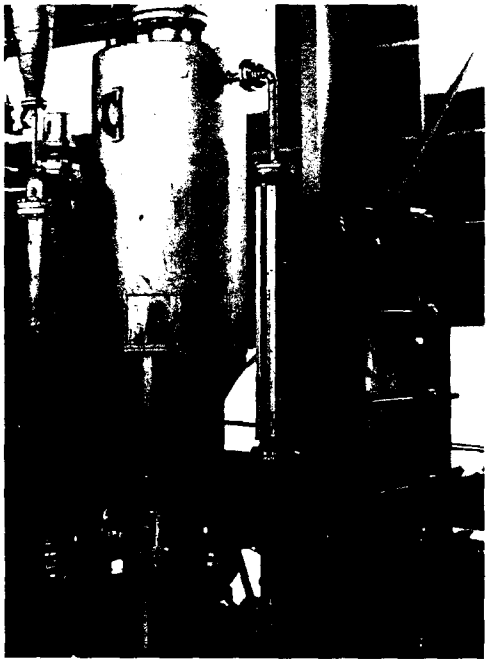

Fig. 3 Plate type evaporator (right) with drain separator (left) at the "Imari 2" OTEC plant

generator and pumps, which are interconnected by pipe lines. Warm surface water is used to evaporate a working fluid, such as Freon 22, in the evaporator. The dry Freon 22 vapor then expands in a turbine to produce power. Finally, cold subsurface water is used to condense the Freon 22 vapor in the condenser. The ultimate purpose of OTEC plant control is to provide stable power efficiently by appropriately regulating the seawater flow rates and the working fluid flow rate under conditions of continually changing seawater temperatures. Figure 2 shows the entire view of the "Imari 2" OTEC plant at Saga University.

The control objective, in this study, is to find a process input signal which will produce an appropriate working fluid flow rate from the working fluid pump, so that the heat rate of the working fluid Q_F at the evaporator will behave according to a desired value. The controlled process consists of the plate type evaporator and the working fluid pump. Figure 3 illustrates the plate type evaporator at the "Imari 2" OTEC plant. The plant must also be equipped with an input signal part and a detection part. The digital controller part consists of a computer (TOSBAC 600) equipped with analog-digital (A/D) converters and a digital-analog (D/A) converter.

The digital control system for working fluid flow rate, depicted in Fig. 4, consists of the OTEC plant side and the digital controller side. The two sides are connected by A/D converters and a D/A converter, and they have a symmetric relationship at the converters (Fig. 4) between a real and a mirror image. Amplifiers in the OTEC plant side are used to standardize each of the analog values to the restriction of the A/D converters (0–10.24 V) and to that of the D/A converter (0–10.24 V) respectively. The digital controller side consists of the series combination of the following blocks: a detection characteristics part, an adaptive control part, and an input signal characteristics part. The procedure used in designing the digital controller side is summarized in the following four steps: (i) modeling of the control objective, (ii) application of adaptive control theory, (iii) characterization of the detection part and input signal part, and (iv) construction of the controller.

2.2 Modeling of the control objective

The controlled process, which consists of the evaporator and the working fluid pump, is assumed to be modeled by a pulse transfer function of the first order as

$$Q_F(k)=\{(b_0+b_1z^{-1})/(1+a_1z^{-1})\}U(k)+W(k) \quad (1)$$

where the process input U(k) is the input signal for the working fluid pump, and the process output $Q_F(k)$ is the heat rate of working fluid; W(k) represents a process disturbance, k the k-th stage of the sampling period, z^{-1} a backwards shift operator, and (a_1, b_0, b_1) unknown parameters of the process. Those parameters are estimated on-line by a recursive identification algorithm.

2.3 Adaptive control part

The adaptive control part, which is a mirror image of the controlled process in Fig. 4, comprises combinations of a recursive identification algorithm and an easy-to-control algorithm as follows: the

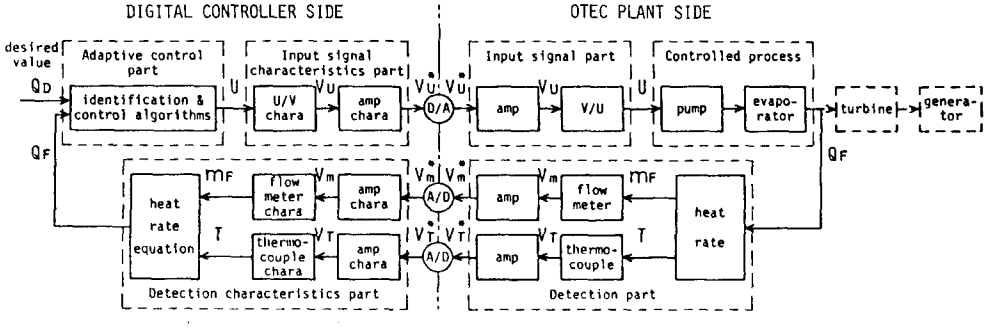

Fig. 4 Digital control system for working fluid flow rate

unknown parameters of the model of the process are estimated on-line by use of the identification algorithm, and an appropriate process input U(k) is determined by the control algorithm using the estimated parameters (a_1, b_0, b_1) thus obtained.

(a) Identification algorithm

We adopt the exponential weighted least squares (EWLS) method [9] as the identification algorithm. The estimated parameters of the process are given by

$$\hat{\mathbf{p}}(k)=[\hat{a}_1(k) \quad \hat{b}_0(k) \quad \hat{b}_1(k)]^T$$
$$=\{I-K(k)\mathbf{z}(k)\}\hat{\mathbf{p}}(k-1)+K(k)Q_F(k), \tag{2}$$

$$C(k)=\{I-K(k)\mathbf{z}(k)\}C(k-1)/\rho, \tag{3}$$

$$K(k)=C(k-1)\mathbf{z}(k)/\{\mathbf{z}(k)^TC(k-1)\mathbf{z}(k)+\rho\} \tag{4}$$

where $\hat{\mathbf{p}}(k)$ is the estimated parameter vector. Both the estimated parameter vector $\hat{\mathbf{p}}(k-1)$ and the estimation matrix C(k-1) on the right side of the above equations have already been determined in the previous stage k-1. The input-output vector $\mathbf{z}(k)$ is the column vector whose elements are the process input and the process outputs as

$$\mathbf{z}(k)=[Q_F(k-1) \quad U(k) \quad U(k-1)]^T. \tag{5}$$

The index ρ is in the range $0 < \rho \leq 1$, and I is the identity matrix.

(b) Control algorithm

We adopt the observer-and-regulator using an extended model [10] as the control algorithm. Arranging the control algorithm, we obtain a process input for the next stage k+1 as

$$U(k+1)=r_1(k)\hat{x}(k+1)+r_2(k)\sum_{i=-\infty}^{k}\{Q_F(i)-Q_D(i)\}. \tag{6}$$

The value $Q_D(i)$ represents a desired output value, and the variable $\hat{x}(k+1)$ is calculated by the observer as follows:

$$\hat{x}(k+1)=-\hat{a}_1(k)\hat{x}(k)+\{\hat{b}_1(k)-\hat{a}_1(k)\hat{b}_0(k)\}U(k)$$
$$-r_3(k)\{Q_F(k)-\hat{x}(k)-\hat{b}_0(k)U(k)\}. \tag{7}$$

The parameters ($r_1(k)$, $r_2(k)$, $r_3(k)$) of the observer-and-regulator in the above equations are

$$r_1(k)=\{\lambda_1+\lambda_2+\hat{a}_1(k)-1-\hat{b}_0(k)r_2(k)\}$$
$$/\{\hat{b}_1(k)-\hat{a}_1(k)\hat{b}_0(k)\}, \tag{8}$$

$$r_2(k)=(\lambda_1+\lambda_2+\lambda_1\lambda_2-1)/\{\hat{b}_0(k)-\hat{b}_1(k)\}, \tag{9}$$

$$r_3(k)=\mu+\hat{a}_1(k) \tag{10}$$

where λ_1 and λ_2 are poles of the regulator, and μ is a pole of the observer. These poles must be selected appropriately by the designer beforehand. Since the control parameters $r_1(k)$, $r_2(k)$ and $r_3(k)$ are calculated using the estimated parameters of the process $\hat{\mathbf{p}}(k)$, the control algorithm can adapt properly to the process even under varying conditions.

(c) Initial condition

The initial value of the estimated parameter vector is necessary as the initial condition for the identification algorithm. Before digital control commences, the initial value is calculated using input and output data based on the exponential weighted least squares of batched type as follows:

$$\hat{\mathbf{p}}(0)=\{\sum_{i=1-N}^{0}\rho^{-i}\mathbf{z}(i)\mathbf{z}(i)^T\}^{-1}\sum_{i=1-N}^{0}\rho^{-i}\mathbf{z}(i)Q_F(i). \tag{11}$$

This algorithm is equivalent to the algorithm of an on-line type, equations (2) through (4).

2.4 Characterization of detection part and input signal part

(a) Detection characteristics part

The heat rate of the working fluid given at the evaporator is determined by the working fluid flow rate and the working fluid temperatures. The working fluid flow rate is detected by an electro-oscillation type flow meter and an amplifier. The characteristics of the amplifier are expressed as

$$V_m=V_m^* \quad [V] \tag{12}$$

and the relation between the flow rate m_F and the voltage V_m is given by

$$m_F=0.833V_m \quad [kg/s]. \tag{13}$$

The working fluid liquid temperature T_{FI} at the inlet and the working fluid vapor temperature T_{VO} at the outlet of the evaporator are detected by thermo-couples and amplifiers. The amplification factor is 5000, and the characteristics of the amplifiers are written

$$V_T=0.200V_T^* \quad [mV]. \tag{14}$$

The thermocouples are characterized by the following polynomial equations of V_T based on the least squares method:

$$T_{FI}=2.116\times10^{-2}+2.506\times10^{1}V_{TF}+6.151\times10^{-1}V_{TF}^2$$
$$-8.173\times10^{-1}V_{TF}^3+1.805\times10^{-1}V_{TF}^4 \quad [°C], \tag{15}$$

$$T_{VO}=-6.700\times10^{-3}+2.539\times10^{1}V_{TV}-2.065\times10^{-2}V_{TV}^2$$
$$-4.520\times10^{-1}V_{TV}^3+1.114\times10^{-1}V_{TV}^4 \quad [°C]. \tag{16}$$

The heat rate of working fluid Q_F in the evaporator is determined by the working fluid flow rate m_F and the specific enthalpy difference between $h(T_{VO})$ and $h(T_{FI})$ as follows:

$$Q_F=m_F\{h(T_{VO})-h(T_{FI})\} \quad [kW]. \tag{17}$$

The characteristics of the specific enthalpies are formulated by polynomial equations based on the least squares method for the data in the Freon 22 Table [8] as

$$h(T_{VO})=4.047\times10^{2}+3.592\times10^{-1}T_{VO}$$
$$-1.429\times10^{-3}T_{VO}^2-1.788\times10^{-5}T_{VO}^3 \quad [kJ/kg], \tag{18}$$

$$h(T_{FI})=2.000\times10^{2}+1.158\times10^{0}T_{FI}$$
$$+1.519\times10^{-3}T_{FI}^2+9.895\times10^{-6}T_{FI}^3 \quad [kJ/kg]. \tag{19}$$

(b) Input signal characteristics part

The relation between the pump input voltage V_U and the working fluid flow rate U (the process input) is

determined by a polynomial equation based on the least squares method as

$$V_U = -6.000\times10^{-2} + 6.286\times10^{0}U - 1.606\times10^{-1}U^2 \quad [V]. \tag{20}$$

The characteristics of the amplifier used here are expressed as

$$V_U^* = 0.667 V_U \quad [V]. \tag{21}$$

2.5 Construction of the digital controller

The digital controller is constructed by a computer (TOSBAC 600) equipped with A/D converters and a D/A converter. The output signals of the OTEC plant are transmitted to the computer through the A/D converters. The converted digital signals are processed by the series combination of the program: detection characteristics part (12)-(19), adaptive control part (2)-(11), and input signal characteristics part (20)-(21). The processed signals are again transmitted to the OTEC plant side through the D/A converter. Those algorithms are iterated through the implementation of the working fluid flow rate control period.

3. Bursting Phenomena and Countermeasures

3.1 Control results

We investigate two kinds of control using the digital controller described in the previous chapter for the "Imari 2" OTEC plant. In the experiments, warm fresh water heated by a boiler and cold fresh water cooled by a refrigerating machine were used instead of warm surface seawater and cold subsurface seawater. The turbine-generator was disconnected from the OTEC plant for the purpose of the experiments.

(a) Satisfactory control result

In the first control experiment, we investigated the digital control of working fluid flow rate under constant conditions; the index of EWLS ρ was 0.95. Other conditions for the experiment were as follows:

desired output value $Q_D(k)$, 250 Mcal/h (291 kW)
warm water flow rate m_H, 20 t/h (5.56 kg/s)
warm water temperature T_H, 30 °C
cold water flow rate m_C, 80 t/h (22.22 kg/s)
cold water temperature T_C, 10 °C
sampling period, 5 s
number of control stages N, 90
poles of the regulator λ_1 λ_2, 0.7 0.7
pole of the observer μ, 0.5
initial value $\hat{p}(0)$, $[-0.115\ -39.11\ 252.20]^T$
initial value C(0), diag(0.0100, 1752, 1752)
(diag: diagonal matrix)
initial value $z(1)$, $[0\ \ 0\ \ 0]^T$
initial value $\hat{x}(1)$, 160 Mcal/h (186 kW)
initial condition $\sum_{i=-\infty}^{0} \{Q_F(i)-Q_D(i)\}$, 250 Mcal/h (291 kW)

Figure 5-A shows the input U(k), the output $Q_F(k)$ of the digital control. As seen from Fig. 5-A, the output $Q_F(k)$ approached the desired output value $Q_D(k)$ in 80 s and maintained its value. The estimated parameters $\hat{p}(k)$ are shown in Fig. 5-B; they keep almost constant values for the whole control interval.

(b) Bursting control result

In the second control experiment, the index of EWLS ρ was changed from 0.95 to 0.90. Other conditions were the same as those adopted for the previous experiment except that the number of control stages, N, was 100. The value $(1-\rho)$ shows the rate of innovative term of the current measurement $Q_F(k)$ in parameter updating of the identification algorithm (2),[9]. The conditions in the second experiment will give more sensitive adaptation to a change of

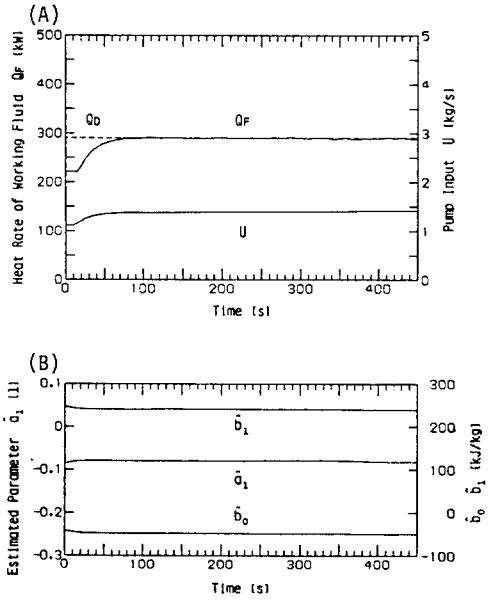

Fig. 5 The process input, output (A), and the estimated parameters (B) in the first control experiment (constant conditions, ρ=0.95)

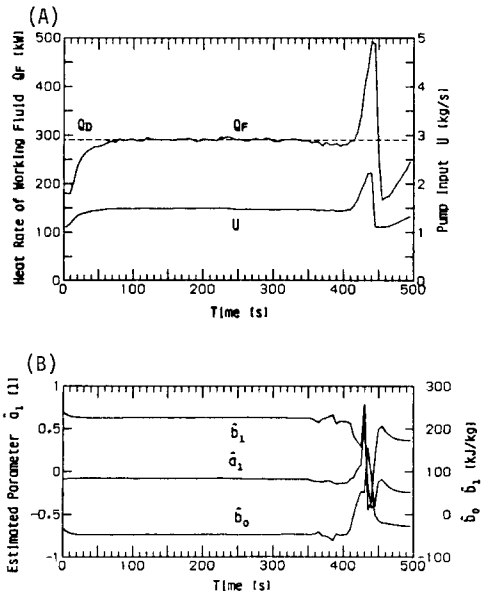

Fig. 6 The process input, output (A), and the estimated parameters (B) in the second control experiment (constant conditions, ρ =0.90)

circumstances. Figure 6 shows the input U(k), the output $Q_F(k)$ and the estimated parameters $\hat{\mathbf{p}}(k)$ in the second control experiment. As seen from Fig. 6, the output $Q_F(k)$ approached the desired value $Q_D(k)$ in 60 s, maintained its value until 350 s, and then diverged. This bursting phenomenon was caused by the absence of persistency of excitation in the identification algorithm [11]. To circumvent this difficulty, the identification algorithm must be modified as described in the next section.

3.2 Stopping-and-starting rule

To avoid bursting phenomena, we monitor the information matrix G(k), inversion of the estimation matrix C(k), during the implementation of the control period, and detect the rank of the information matrix by using the Gram-Schmidt orthonormalization. We calculate the information matrix G(k) as

$$G(k)=Y(k)R(k)Y(k)^T,$$
$$Y(k)=[\mathbf{z}(1) \cdots \mathbf{z}(k)], \qquad (22)$$
$$R(k)=\mathrm{diag}(\rho^{k-1}, \cdots, \rho^0).$$

Using the j-th column vector $\mathbf{g}_j(k)$ of G(k), we obtain the vector $\mathbf{d}_j(k)$ as

$$\mathbf{d}_j(k)=\mathbf{g}_j(k)-(\hat{\mathbf{d}}_{j-1}(k),\mathbf{g}_j(k))\hat{\mathbf{d}}_{j-1}(k),$$
$$\hat{\mathbf{d}}_{j-1}(k)=\mathbf{d}_{j-1}(k)/|\mathbf{d}_{j-1}(k)|, \qquad (23)$$
$$\mathbf{d}_0(k)=0 \quad (j=1,2,3)$$

where (,) represents the inner product and $|\ |$ represents the Euclidian norm. If one out of three conditions

$$|\mathbf{d}_j(k)| < \varepsilon_1 \quad (j=1,2,3) \qquad (24)$$

is satisfied, the rank of the information matrix is regarded as being reduced and the identification algorithm (2)–(4) stops. In a stopping state of the parameter updating, if the conditions

$$|\mathbf{d}_j(k)| > \varepsilon_2 \quad (j=1,2,3) \qquad (25)$$

are satisfied for all j, the rank of the information is regarded as being recovered in full, and the identification algorithm restarts. The values ε_1, ε_2 are determined by the designer before the algorithm commences. The above procedure refers to the stopping-and-starting rule for identification.

3.3 Results using the stopping-and-starting rule

We investigate two kinds of digital adaptive control experiments using the stopping-and-starting rule.

(a) Control result (constant conditions)

In the third control experiment, we investigate the digital control of working fluid flow rate by means of the stopping-and-starting condition under constant conditions, the same as that of the second experiment. The threshold values ε_1 and ε_2 were both set at 0.1. Figure 7 shows the input U(k), the output Q(k) and the estimated parameters $\hat{\mathbf{p}}(k)$ in the third experiment. As seen from Fig. 7, the output $Q_F(k)$ approached the desired value Q_F, and maintained its value until the last stage. The algorithm of the identification stopped at 165 s and did not restart because the control conditions were kept constant.

(b) Control result (variable desired output value)

In the fourth control experiment, the desired output value $Q_D(k)$ was changed from 250 Mcal/h (291 kW) to 300 Mcal/h (349 kW) at a time of 250 s. Other conditions were the same as those adopted for the third experiment. Figure 8 shows the input

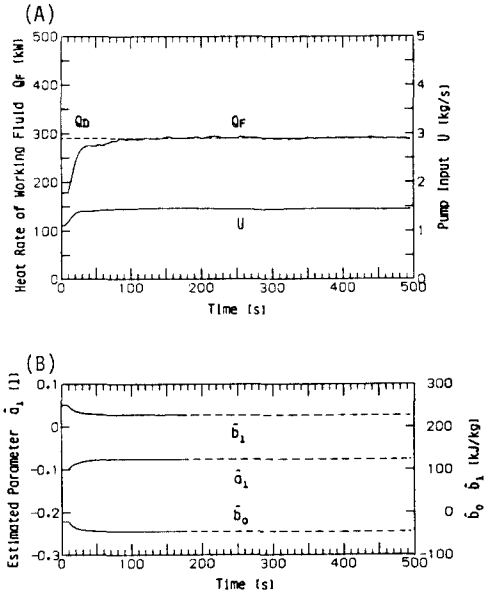

Fig. 7 The process input, output (A), and the estimated parameters (B) in the third control experiment (constant conditions, ρ=0.90, with the stopping-and-starting rule)

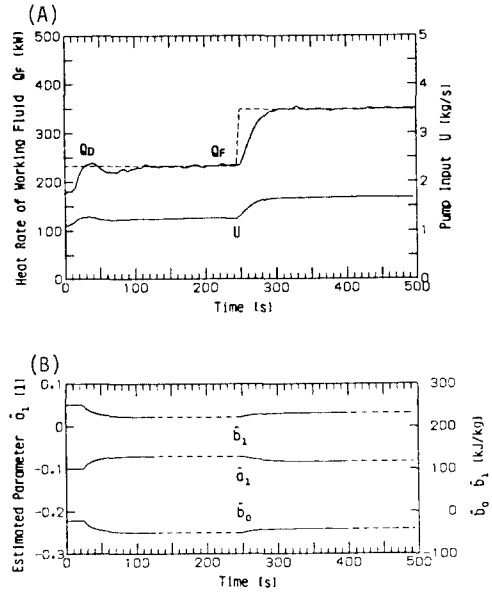

Fig. 8 The process input, output (A), and the estimated parameters (B) in the fourth control experiment (variable desired output value, ρ=0.90, with the stopping-and-starting rule)

$U(k)$, the output $Q_F(k)$, and the estimated parameters $\hat{p}(k)$. According to the stopping-and-starting rule (22)-(25), the algorithm of the identification stopped at 120 s and restarted at 255 s. It may be seen that the process output $Q_F(k)$ behaves appropriately according to the variable desired output value $Q_D(k)$, and that the estimated parameters adapt to the system under the changed conditions.

4. Discussion

(a) Significance

The innovative feature of this study was construction of a digital control system and the implementation of the digital control of working fluid flow rate for the real pilot OTEC plant. In circumventing identification bursting phenomena during periods of absence of persistency of excitation, the stopping-and-starting rule for identification was derived and was used for the working fluid flow rate control. The process output of the digital control behaved appropriately according to a desired output value under changing conditions by use of the digital adaptive controller. The advantages of using digital controllers in general are summarized as follows:

(i) Any adaptive control algorithm can be selected by changing the program of the adaptive control part, whereas for analog-type control, such as the PID controller, this is rather difficult to do once the controller has been attached to the plant.

(ii) Linearity for detection characteristics and for input signal characteristics is not necessarily requisite. The polynomial equations for the characteristics, determined by the least squares method, need only be programmed in the computer.

(b) Remarks

(i) The heat rate of working fluid at the evaporator was calculated by equation (17). A more reliable calculation might be possible by using m_V (working fluid vapor flow rate) instead of m_F (working fluid liquid flow rate) adopted here.

(ii) The process model (1) used here had the structure of the first order. A more appropriate order of the process model might be found by using another technique, such as AIC (Akaike's Information Criterion) [12].

(iii) The values of the poles λ_1, λ_2, μ in the control algorithm and the value of the index ρ in the identification algorithm were selected *a priori* by computer simulation before the control experiments. More appropriate values might be determined through further experimental investigation.

(iv) For an adaptive control theory, we adopted the exponential weighted least squares method as an identification algorithm and the observer-and-regulator as a control algorithm. Other adaptive control theories, such as the MRACS (Model Reference Adaptive Control System) [6], could also be applied simply by changing the program of the adaptive control part.

Acknowledgments

The authors are grateful to Dr. T. Nakaoka (lecturer), Mr. S. Nishida (research assistant), and Mr. N. Egashira (postgraduate student, now with Taku technical high school) of Saga University for their useful comments and help in the experiments, and to Dr. G. Jember of Saga University for revising the English in this paper.

References

[1] J.A. D'Arsonval, Utilization des forces naturelles: Avenir de l'electricite, La Revenue Scientifique, Sept. 17, pp.370-372, (1881)

[2] H. Uehara, H. Kusuda, M. Monde, T. Nakaoka, T. Masuda and M. Nakahara, Model of Ocean Thermal Energy Plant-Shiranui 3, Proc. 5th OTEC Conf., pp.V117-146, (1978)

[3] H. Uehara, Introduction to OTEC, Ohm, (in Japanese), (1982)

[4] W.L. Owens, OTEC Plant Response and Control Analysis, ASME Journal of Solar Energy Engineering, Vol.104, Aug. pp.208-215, (1982)

[5] K.J. Åström, V. Borisson, L. Ljung and B. Wittenmark, Theory and Applications of Self-Tuning Regulators, Automatica, Vol.13, pp.457-476, (1977)

[6] I.D. Landau, A Survey of Model Reference Adaptive Techniques - Theory and Applications, Automatica, Vol.10, pp.353-379, (1974)

[7] M. Nakamura, N. Egashira and H. Uehara, Digital control of working fluid flow rate for an OTEC plant, ASME Journal of Solar Energy Engineering, Vol.108, May pp.111-116, (1986)

[8] JAR., Thermophysical Properties of Refrigerants (R22), (in Japanese), (1982)

[9] M. Nakamura, Relationship Between Steady State Kalman Filter Gain and Noise Variances, Int. J. Systems Sci., Vol.13, No.10, pp.1153-1163, (1982)

[10] K. Furuta, Digital Control and Control Theory, Computrol, No.2, (in Japanese), pp.16-25, (1983)

[11] B.D.O. Anderson, Adaptive systems, Lack of persistency of excitation and bursting phenomena, Automatica, Vol.21, No.3, pp.247-254, (1985)

[12] H. Akaike, A New Look at the Statistical Model Identification, IEEE Trans. Autom. Control, Vol.AC-19, No.6, pp.716-723, (1974)